OXFORD JOURNAL
OF STUDENT
SCHOLARSHIP

Drone Swarm Data Transfer in 3D environments with the effect of Crosswinds using Ant Colony Optimization whilst optimising link quality, delay, and energy usage

Vedansh Gupta
vedanshgupta254@gmail.com

ABSTRACT

UAV swarms generally rely on multi-hop communication systems to perform remote sensing and relay-based tasks. These communication systems involve 3D geometry, radio signal propagation, and various physical and environmental constraints. This paper presents a 3D Ant Colony Optimisation-based routing model that optimises link quality, energy consumption, and delay while accounting for obstructions and crosswinds. In the present study, the proposed model extends on previous 2D studies by incorporating variability in drone altitudes, line of sight blockages caused by buildings, roof-grazing penalties, and crosswind based propulsion energy modelling. The simulations are conducted in both a realistic urban environment as well as an open environment, without any buildings using MATLAB with the objective to optimise all parameters and constraints. The results demonstrate that urban interferences and crosswinds can alter the optimal routing path, and in some cases improve energy efficiency, and reduce delays due to the wind shielding effect from buildings and the overall shorter inter-drone distances that enables more efficient routing. Additionally, further analysis also reveals linear relationships among key parameters including link quality, delay, and energy consumption, and identifies scenarios in which urban environments outperform open environments. These findings highlight the importance of integrating a 3D environmental structure and atmospheric effects such as crosswinds into multi-objective routing models to precisely optimize UAV swarm communication systems in real-world remote sensing applications.

Keywords: 3D routing, Ant Colony Optimization, Drone swarms, Multi-hop Communications, Unmanned Aerial Vehicles, Urban Environment

INTRODUCTION

Unmanned Aerial Vehicles (UAVs), commonly referred to as drones, have emerged as an important platform for remote sensing, communication relays, and data transfer across a wide range of civilian and military applications. In recent years, drone swarms have gained significant attention due to their potential to extend communication coverage, improve spatial communication, and execute effective communication within the swarm in complex environments. These characteristics make UAV swarms especially suitable for applications such as Relay and networking [8] which comprises the primary aim of the current research. In such scenarios, data packets and payloads collected by distributed drones are transmitted from a remote location to the central hub. Another crucial application of drone swarms is in Military and reconnaissance operations [3] where these are employed for surveillance in various regions that may be inaccessible for human pilots. Additionally, UAVs can also be used in disaster-stricken areas [4] for mapping purposes, locating victims, etc. Other applications of drone swarms include environmental monitoring [5] , agriculture and farming [6], infrastructure inspection and maintenance [7], entertainment purposes [9], and package delivery systems [10].

Despite multiple advantages and plethora of applications in various fields, one of the primary challenges in UAV swarm deployment is the execution of efficient multi-hop data communication strategies, where the information collected by individual drones must be transmitted to the sink node. Unlike traditional communication networks, UAV communication networks are highly sensitive to environmental conditions, constrained by limited on-board energy resources, and inherently operate in 3D spaces. Therefore, routing decisions must involve balancing objectives such as link quality, communication delay and energy consumption, while being able to adapt to dynamic network topologies and varying propagation conditions.

Previous research has extensively demonstrated UAV routing and drone swarm communication enhancement using heuristic and bio-inspired algorithms, especially the Ant Colony Optimisation algorithm (ACO). The ACO algorithm utilises probabilistic path exploration and pheromone levels to identify efficient routes, making these well-suited for drone swarm optimisation.

However, the existing literature still contains some research gaps and unmet need. First, significant research in UAV routing is conducted in 2D environments, which fail to account for altitude variation, vertical obstacles, and flight dynamics commonly encountered in urban environments. Second, obstructions such as buildings are often modelled in a simplified manner, despite buildings having a significant impact on link quality and the overall path selection. Lastly, atmospheric effects are rarely considered into such routing models despite an effect on energy usage contributing to flight stability.
These gaps must be addressed to ensure the applicability of drone swarms to real world remote sensing scenarios, where UAV swarms are likely to be deployed in complex environments characterised by environmental effects and physical obstructions.

In an urban environment, routing decisions are likely to be influenced by 3D spacing, radio propagation, energy availability and consumption for each hop, obstacles such as buildings, and atmospheric effects such as crosswinds. Buildings have the potential to obstruct line-of-sight communication links, force path deviations, and introduce diffraction losses, due to bending of the radio waves around obstacles leading to reduced link quality [16]. Crosswinds, on the other hand, have a significant effect on the energy usage to

maintain stability when suspended. Ignoring such effects may lead to suboptimal routing decisions and lower system efficiency.
The present research aims to develop a realistic UAV swarm routing framework that integrates 3D modelling, communication metrics, energy efficiency, building obstructions, and crosswind effects to enable optimal routing decisions. The primary objective of the current work is to holistically optimise link quality, energy consumption, and communication delay within a unified 3D ACO-based routing model to suggest the most suitable path that explicitly accounts for crosswinds and building obstructions.

MATERIALS AND METHODS

2.1 Ant Colony Optimization Algorithm

The ACO algorithm is a heuristic technique that utlilises artificial ants that constantly travel through all the different paths possible until they find the most efficient path. The best possible path is determined using Equation 1 [2]. This is the original ACO algorithm where the probability of selecting a path from i to j is given by analysing two main factors: pheromone level and visibility represented by P and V respectively. They are given different importances/weightings using the alpha and beta variables. The equation is a probability distribution which analyses the probability of all the possible paths given by the denominator of the equation with the use of summation notation describing the sum of probabilities of all the paths. The $k \in Rd$ part of the summation represents the paths that have not been visited by the drone yet.

$$P_{ij} = \frac{(P_{ij})^{\alpha} \times (V_{ij})^{\beta}}{\sum_{k \in R_d} (P_{ik})^{\alpha} \times (V_{ik})^{\beta}} \tag{1}$$

As the virtual ants travel these paths, they release a substance called pheromone. Paths that are more commonly travelled would have a greater concentration of pheromone which helps other ants that traverse the path later on to pick the most efficient option. In order for the ants to forget the inefficient paths, the pheromone needs to evaporate over time and is given by Equation 2. This is done after each iteration of the algorithm.

$$P_{ij} = (1 - \rho) P_{ij} + \rho \Delta P_{ij} \tag{2}$$

The P_{ij} signifies the amount of pheromone given on the edge between point i and point j. The $(1-\rho)$ is the decay function that gradually reduces the pheromone level on the path over time for a value of ρ in the interval [0,1] . The $\rho\Delta P_{ij}$ represents the new pheromone that is put onto the path with each iteration of the algorithm.

The ACO algorithm is used to best navigate through different arrangements of buildings while picking the best paths so that energy usage per communication hop is minimised, the link quality is maximised and the delay is minimised. The ACO will also be active when the drones are placed in a scenario with wind coming from a particular direction that can have an impact on the above parameters and needs to be accounted for when the drone picks the best path.

2.2 P-BIOSARP Autonomous Routing Protocol

Power-Aware Biologically Inspired Secure Autonomous Routing Protocol (P-BIOSARP) [1] modifies Equation 1 and considers three key factors which affect drone data transfer: link quality, delay and remaining energy. They are represented by the variables α, β and δ respectively. In P-BIOSARP, the maximum weightage is given to energy usage or the remaining energy parameter as the algorithm is considered power-aware. Equation 3 below gives the principal P-BIOSARP algorithm. The w variables in the exponents represent the respective weightages. Just like in the original ACO algorithm, this P-BIOSARP protocol is based on probabilities and finds the probability of taking a certain path and compares it to all the other unexplored paths as represented by the summation notation.

$$\mathscr{P}_{cn}(\varepsilon) = \frac{\left[\alpha_{cn}(\varepsilon)\right]^{max(w\alpha)} \cdot \left[\beta_{cn}(\varepsilon)\right]^{min(w\beta)} \cdot \left[\delta(\varepsilon)\right]^{min(w\gamma)}}{\sum_{k \in cn}^{\infty}\left[\alpha_{cn}(\varepsilon)\right]^{max(w\alpha)} \cdot \left[\beta_{cn}(\varepsilon)\right]^{min(w\beta)} \cdot \left[\delta(\varepsilon)\right]^{min(w\gamma)}} \quad \textbf{(3)}$$

2.3 3D modelling

A 3D model of the environment was developed using Matlab. First, a 100x100m 2D environment with 10 drones was developed. Each drone was represented as a circle and labelled as D1, D2, D3, etc. Later, buildings of different sizes were added and represented by grey rectangles.

To expand the simulation to 3D, a Z axis is added, which also goes up to 100m. This means the terrain is now a 100x100x100m region. The building's dimensions remain the same except for an additional height parameter. The height is randomised to a value between 30-80 meters to simulate a real-life scenario in a city. The shape of the drones become smaller red colour rectangular prisms to closely match the shape of real drones. The altitude of the drones is set between 30-60 meters for variation.

2.4 The environmental constraints

The environmental constraints involved the area in which the simulations are taking place. The dimensions of the region is 100x100x100 meters and is modelled to take place in a city environment with many buildings. There will be 10 drones in the region and each drone will be hovering at a random height between 30 and 60 meters. To get the distances between drones, the simulation uses the euclidean distance matrix between each drone pair(d_{ij}).

2.5 The building constraints

The building constraints involve the number of buildings in the simulation which has been kept to 15. Each building's length and width is randomised between 8 and 14 meters and the height of the buildings are randomised between 30 to 80 meters. Buildings do not overlap in any way in the 3D environment. For the building obstruction constraints, the model identifies an obstruction when a straight line of sight path is blocked by a building. This results in the drone having to climb up to the top of the building plus a 5 meter clearance distance and then back down to the straight line of sight path. This causes there to be a new detour distance rather than the straight line distance. There is also a 2db roof-grazing penalty being applied due to diffraction and scattering of links near the top of buildings leading to attenuation of the link quality. Essentially the link quality reduces and the communication delay and communication energy rise.

2.6 The radio and communication constraints

The radio and communication constraints involve the transmitter and channel parameters. The transmit power (P_{tx}) is set to 20 decibel-milliwatts, the antenna gains, as seen in Equation 4 ,(G_{tx} and G_{rx}) are set to 2dBi, the carrier frequency is set to 2.4GHz, the noise floor is set to -100dBm, and the receiver sensitivity is kept at -90dBm. As depicted in equation 5, the free space path loss is used to find the transmission loss and later the link quality. Each of the open spaces and the environment with buildings will have their own mappings due to different link qualities.

2.7 The energy constraints

For the energy constraints, the model assumes that the total energy is composed of the sum of the communication, propulsion and computational energies. The base propulsion cost, given by the variable α_E, is set at 0.8 joules per meter, and the propulsion energy is based on the factors such as wind and airspeed. The nominal airspeed($\mathbf{V}_{nominal}$) is kept at 10m/s. The energy is also influenced by the crosswinds acting on the drone where crosswinds result in 20% extra energy usage when at full force. The buildings also reduce the impact of the wind by creating a shielding effect of 50%. For the communication energy, the model assumes that the data payload is 1MB per link and the channel bandwidth is 20MHz, and the computational energy has a fixed cost of 0.2J per communication hop. For the ease of comparison, the energy usage will be converted into a scale from 0-1.

2.8 The wind constraints

The wind constraints involve the speed of the crosswind which is set to 5m/s and the direction which is set from east to west or 180º. As mentioned in the energy constraints, the crosswind affects propulsion energy and adds a penalty due to reduction in stability of the drone.

2.9 Ant Colony Optimization constraints

Lastly for the Ant Colony Optimization constraints, the model assumes there are 30 ants and the optimal path is determined through 50 interactions of the algorithm. The pheromone importance (α) is set to 1, and the heuristic importance(β), based on link quality, delay and energy usage, is given an importance of 5. The pheromone evaporation rate(ρ) is set to 0.5.

2.10 To study the effect of various constraints on link quality:

The methodology involves calculating the first of the parameters influencing the efficiency of each individual drone: the link quality. This can be done using the Free Space Path Loss (FSPL) algorithm [12] using the Equation 4, where P_{rx} is the power received, P_{tx} is the power transmitted, G_{tx} and G_{rx} are the transmitting and receiving antenna gains respectively, λ is the wavelength of the signal, and d is the distance between the antennas of any two drones.

$$P_{rx} = P_{tx}\left(\frac{G_{tx}G_{rx}\lambda^2}{(4\pi d)^2}\right) \tag{4}$$

Section 2.3 from this paper [13] highlights the rearranged form for the transmission loss using distance and wavelength. The equation in this paper uses the distance in km but changing the distance in the formula to meters we get Equation 5 below. This is done by subtracting $20\log_{10}(1000)$ from 32.45 giving -27.55. In Equation 5, d_m is the distance between the drones in meters and f_{MHz} is the frequency of the signal between the drones in MegaHertz.

$$FSPL(dB) = 20\log_{10}(d_m) + 20\log_{10}(f_{MHz}) - 27.55 \tag{5}$$

There is an equation for the received power P_{rx}(dBm) of a drone when it receives data from another drone in the region. This can be done by subtracting all the power losses from the power gains including the free space path loss calculated from Equation 5. P_{tx} , G_{tx} , L_{tx} , G_{rx} , L_{rx} represent the transmitted power, transmitter antenna gain, transmitter cable loss, receiver antenna gain, and receiver cable loss, respectively. The equation for received power, P_{rx}(dBm), is given by Equation 6.

$$P_{rx}(dBm) = P_{tx}(dBm) + G_{tx}(dBi) - L_{tx_{cable}}(dB) + G_{rx}(dBi) - L_{rx_{cable}}(dB) - FSPL(dB) \tag{6}$$

Next, the signal to noise ratio of the system is calculated which compares the strength of the signal between two drones to the noise in the background. This ratio can be used to convert the link quality value into a number between 0 and 1 where 0 represents a very weak link quality and 1 represents a very strong link quality.

2.11 To study the effect of various constraints on energy usage:

The total energy used between two drones from point i to j are dependent on two main energy sub-categories: propulsion energy and communication energy. The propulsion energy allows the drone to remain in the air and gives the drone the upthrust force; it is also affected when the drone travels to send data. The communication energy is the energy required to actually send the data from one drone to another. Together, when summing up these energies, the total energy is obtained as shown in Equation 7 below. There is also a fixed computational energy also included in the equation below to conduct processing and run algorithms such ACO which we consider γE. γE is kept at a fixed cost of 0.2J per communication hop.

$$E_{total}(i,j) = E_{propulsion}(i,j) + E_{comm}(i,j) + \gamma E \tag{7}$$

The propulsion energy relies on the distance between two drones and a fixed constant that represents the energy used per meter of travel and uses the unit joules per meter. The constant also needs to be adjusted for the wind that may be acting on the drone. This is because wind, in this case crosswind, can lead to a greater energy usage as the drone needs to invest more of its energy into combatting lateral forces and angle itself so that it can continue on its intended flight path. This constant can be called $\alpha_E^{eff}(i,j)$ and the distance can be called d_{ij}. Equation 8 indicates the relationship that gives the total propulsion energy.

$$E_{propulsion}(i,j) = \alpha_E^{eff}(i,j) \times d_{ij} \tag{8}$$

The wind adjusted fixed energy used per meter term $\alpha_E^{eff}(i,j)$ is computed using Equations 9 and 10 below. α_E is the fixed energy used per meter constant without being adjusted for wind and it will be kept at 0.8J/m. $\mathbf{V}_{nominal}$ is the expected velocity of the drone without any wind and $\mathbf{V}_{actual}$ is the velocity after being affected by wind. Equation 9 builds upon the energy per unit distance idea developed in this paper[15]. The crosswind_penalty just represents the extra small amount of energy needed to keep the drone stable when a crosswind causes it to become off-balance. $\mathbf{V}_{actual}$ is essentially just the magnitude of the wind velocity subtracted from the nominal velocity in a particular direction, denoted by the $\mathbf{d}_{ij}$ vector where the hat notation represents the unit direction vector, as stated by Equation 10. $\mathbf{V}_{nominal}$ is assumed to be 10 meters per second and $\mathbf{V}_{wind}$ is 5 meters per second coming from 180º.

$$\alpha_E^{eff}(i,j) = \alpha_E \times \left(\frac{V_{\mathbf{actual}}}{V_{\mathbf{nominal}}}\right)^2 \times (1 + crosswindpenalty) \tag{9}$$

$$V_{\mathbf{actual}} = \left| \mathbf{V}_{\mathbf{nominal}} \times \widehat{\mathbf{d}_{\mathbf{ij}}} - \mathrm{V}_{\mathrm{wind}} \right| \tag{10}$$

To calculate the propulsion delay, the Equation 11 given below links together the propulsion power P_{prop} and the time taken to travel from point i to j, t_{ij}. These quantities are multiplied as the total energy used for the propulsion for the drone is the power needed per unit time for a certain amount of time t_{ij}.

$$E_{propulsion} = P_{propulsion} \times t_{ij} \tag{11}$$

The below Equation 12 is used to calculate the propulsion power P_{prop} using the aerodynamic drag equation in fluid dynamics. The ρ represents air density in kg/m^3, C_d represents the drag coefficient of the drone, A is the area of the drones frontal region and $\mathbf{V}_{actual}$ is the same as established before.

$$P_{propulsion} = \frac{1}{2}\rho C_d A\left(V_{actual}\right)^3 \tag{12}$$

Similar to the link quality, the energy ($E_{total}(i,j)$) given in Equation 7 above will be converted to a scale from 0-1 for easier comparison in the results section of the paper. The value 0 represents maximum energy used while the value 1 represents minimum energy used in a communication hop between two drones.

2.12 To study the effect of various constraints on communication delay:

The last important parameter to consider in this model is the Delay. This is the amount of time taken for the data to be transmitted from one drone to another. The delay is likely to be higher if the distance between two drones is larger, buildings force the data transmission to take a longer path, worsening of channel quality ,etc , and the delay parameter is closely linked to the link quality parameter. In this paper the delay is split into two sub-parts: the propagation delay(relating to the motion of the drone) and the communication delay.

$$CommDelay_{ij} = \frac{8S}{B\log_2\left(1 + SNR_{lin}\right)LQ_{ij}} \tag{13}$$

Equation 13 indicates how communication delay is calculated in this model. S represents the packet size, B represents the channel bandwidth, SNR_{lin} represents the linear model of the signal to noise ratio and LQ_{ij} is the link quality between two points i and j. This equation is a modification of the Shannon- Hartley theorem [14].

Using Equation 14 below, the propagation delay is calculated. The d_{ij} represents the total distance travelled from point i to j and $\mathbf{V}_{nominal}$ is the nominal velocity of the drone in a certain period. This gives the time taken or delay over a distance moved.

$$PropagationDelay_{ij} = \frac{d_{ij}}{V_{nominal}} \tag{14}$$

To reiterate, when a drone faces an obstruction such as a building, it makes three movements. It moves up, then horizontally across the obstacle, and then back down. This adds to the extra distance travelled which therefore increases the total propagation delay. It is assumed that the drone moves a nominal velocity of 10 meters per second.

2.13 Simulations and Testing

Two simulation scenarios of open and urban environments (with buildings) were created according to the constraints mentioned above. The same random placement of 10 drones was used in both cases for the fair comparison of the routing performance in the same network condition. For every scenario, the routing algorithm was applied to this common network configuration and various performance metrics such as the link quality, propagation delay, communication delay, and normalized energy consumption were measured for each drone. The results reported in the Results section are average values calculated from the 10 drones in each simulation, thus providing a uniform comparison of the overall swarm performance in the two environments.

RESULTS AND DISCUSSION

3.1 2D environment modelling

This subsection highlights the model of the urban environment when in 2D. It showcases the optimal routing path and navigation around buildings.

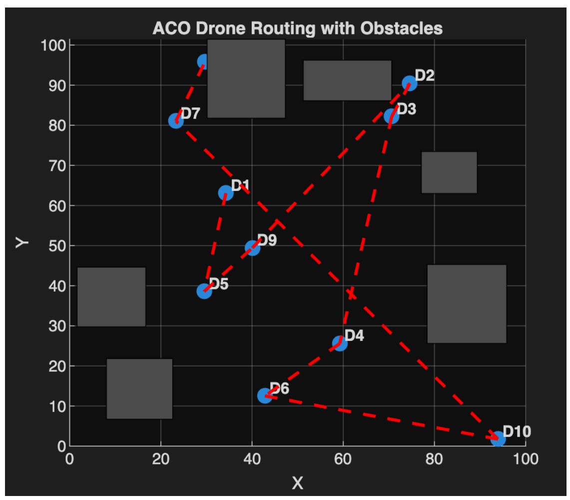

Fig. 1 2D urban environment

In 2D simulation, the red dotted lines represent the best path of the ACO algorithm which is the path taken by the drones to transmit data packets, and the grey squares represent various buildings in an urban environment.

3.2 Moving from 2D to 3D in drone routing and parameter optimisation

This subsection highlights the shift from 2D simulation and routing optimisation as seen in section 3.1 to including a 3rd dimension given by the letter Z.

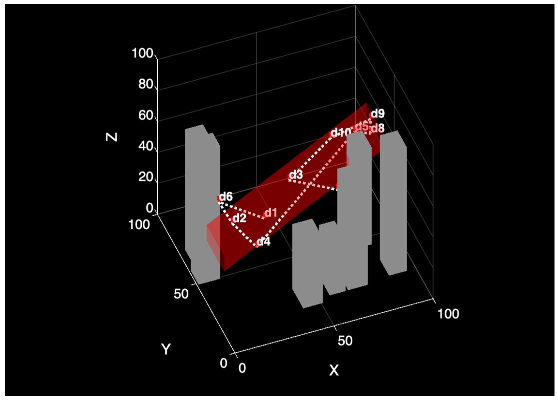

Fig. 2 Shift to 3D for drone routing

The 3D model of the terrain depicted. The red translucent region represents a possible path taken by the crosswind but in the simulations later in the paper, the crosswind approaches from a fixed 180º angle from the west.

3.3 Parameter differences between open and building environments:

The below Figures 3a and 3b depict the results of the model given the above constraints for both with and without buildings. This section compares the paths as well as the link qualities, energy, and delays of both environments. Both models assume that the wind is acting on the drones.

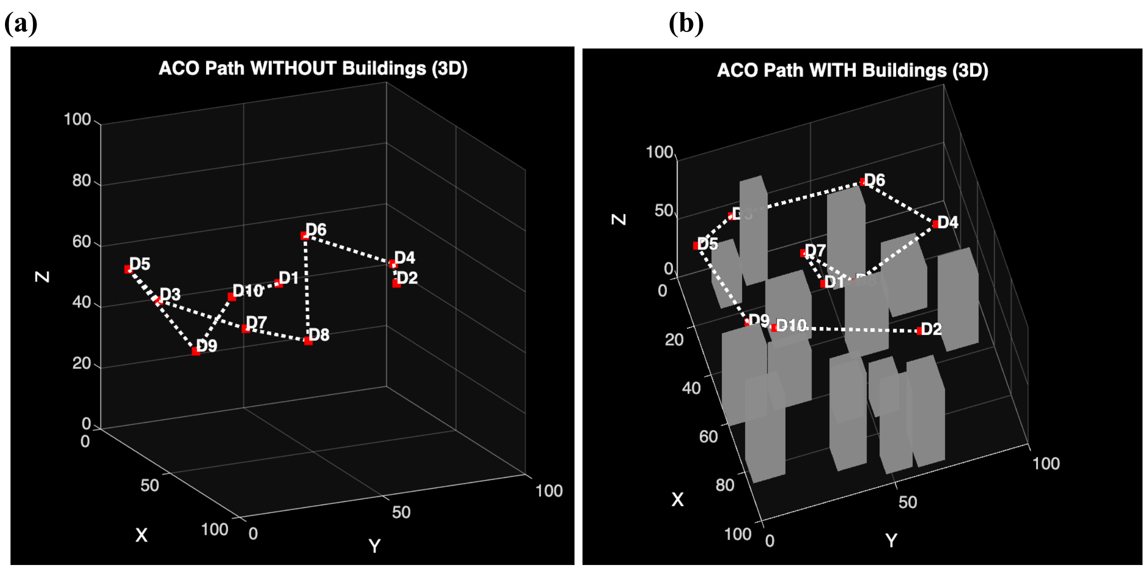

Fig. 3 Parameter routing differences between open and building environments
(a) ACO path without building (b) ACO path with buildings

As seen in the above two simulations, the paths differ substantially. In the open simulation the optimal path goes from D1-D10-D9-D5-D3-D7-D8-D6-D4-D2 while in the building simulation the path goes from D1-D7-D8-D4-D6-D3-D5-D9-D10-D2. These simulations show that the algorithm tends to avoid buildings or obstructions as well as the roof grazing penalty. This can be seen between drones D1 and D10; in the open simulation there was nothing preventing the path between them but in the building simulation a medium height building obstructed the path and resulted in the drone D1 to instead proceed to send data to D7. The reason for this change is likely due to the increase in the signal to noise ratio leading to a lower link quality therefore leading to the geometrically shortest paths being ignored as they become more unreliable.

The below Tables 1 and 2 show the comparisons of the different link qualities, Delays, energy usage, and communication delay for both the open and building environments. The bottom of the tables also present the averages of all the values which allow for better comparison. Table 3 shows the difference between the propagation delay of the two environments in the third column and again provides their mean values.

Table 1. Key Parameters in Open Space environment

Drone	Link Quality	Delay (s)	Energy (norm)	CommDelay (ms)
1	0.780	2.535	0.319	22.5481
2	0.344	4.677	1.000	24.6534
3	0.846	2.881	0.244	22.1177
4	0.536	3.846	0.749	23.7455
5	0.692	3.160	0.016	22.9055
6	0.598	3.395	0.272	23.4401
7	0.889	2.522	0.374	21.6381
8	0.706	2.955	0.169	22.5594
9	0.695	3.044	0.000	22.8799
10	0.822	2.578	0.160	22.2661
Mean	0.691	3.159	0.330	22.8754

Table 2. Key Parameters in Urban environment

Drone	Link Quality	Delay (s)	Energy (norm)	CommDelay (ms)
1	0.794	3.152	0.000	22.8656
2	0.005	7.548	1.000	39.6500
3	0.325	4.443	0.374	26.4439
4	0.342	3.895	0.139	26.2987
5	0.538	3.374	0.366	24.7773

6	0.338	4.529	0.237	26.3448
7	0.848	2.643	0.071	22.2600
8	0.578	3.236	0.213	24.3623
9	0.575	3.240	0.342	24.5068
10	0.241	5.281	0.611	32.4171
Mean	0.458	4.134	0.335	26.9926

Table 3. Propagation delay comparison across both environments

Drone	Delay (With Buildings) [s]	Delay (Open) [s]	Difference [s]
1	3.152	2.535	0.617
2	7.548	4.677	2.870
3	4.443	2.881	1.562
4	3.895	3.846	0.049
5	3.374	3.160	0.214
6	4.529	3.395	1.134
7	2.643	2.522	0.121
8	3.236	2.955	0.282
9	3.240	3.044	0.197
10	5.281	2.578	2.703
Mean	4.134	3.159	0.975

The data across the three Tables show quite a bit of variability between drones in the building environment compared to the open environment. This variability arises from the geometric positions of the drone as some are on straight line paths whilst others require detours involving moving close to buildings and roofs. Also the drones moving with the crosswind are able to move around while expending less propulsion energy. These differences across drones are what lead to variable link qualities, higher delays, and a slight increase in energy usage for certain drones in longer paths.

Analysing the link quality, from Tables 1 and 2, the average link quality goes from 0.458 in the building environment to 0.691 in the open environment. This is due to the extra losses added in obstruction and roof grazing penalties. As the Signal to Noise ratio(SNR) is the difference between the received power and the noise floor level, the SNR decreases as the losses decrease the received power. Some drones are affected more than others such as drone D2 in the building environment as it is both far away from the drone it receives data from and is surrounded by many buildings resulting in a greater worsening of link quality with the drones around it. The actual impact on buildings on the link quality is not always linear, though; buildings disproportionately harm weaker links rather than stronger ones causing an unevenness in the link quality displayed in the table.

With the delay, the propagation delay, as mentioned in Table 3, of the building environment is 4.134 seconds while the propagation delay of the open environment is 3.159 seconds. This is a difference of 0.975 seconds. However, the difference between the communication delays between the two environments is 4.117 milliseconds from the 22.8754 milliseconds in the building environment and the 26.9926 milliseconds in the open environment. The propagation delay increases by a larger amount than the propagation delay and this is likely due to the fact that buildings lead to poorer local links between drones and this leads to longer routes and a greater total travel time. The communication delay increases by a much lower amount as the path changes don't significantly alter the time taken for the radio waves to travel a slightly longer distance. These waves will still travel at $3x10^8$ meters per second.

Additionally, the energy usage between these two environments doesn't change significantly. In the open environment, the average energy usage is 0.330 while in the building environment, the average energy is 0.335. This is likely due to the fact that propulsion energy makes up most of the total energy consumption as compared to communication energy which only consists of the data packet transfers. The propulsion energy refers to the energy that is made up of the drones travelling, and the actual path distance doesn't really change by that much, and the speed at which the data is transferred is also extremely fast. Therefore the actual energy increase is almost 0 when buildings are present.

The link quality, delay, and energy parameters are quite interlinked together. If there is a poor link quality, then there is likely to be a larger communication delay, and if there is longer total delay, then it is likely that more energy would have been spent transmitting the data packets. These relationships have been further explained in sections 3.2, 3.3 and 3.4 of the results.

3.4. Analysis of Normalised Energy vs Link Quality across both environments

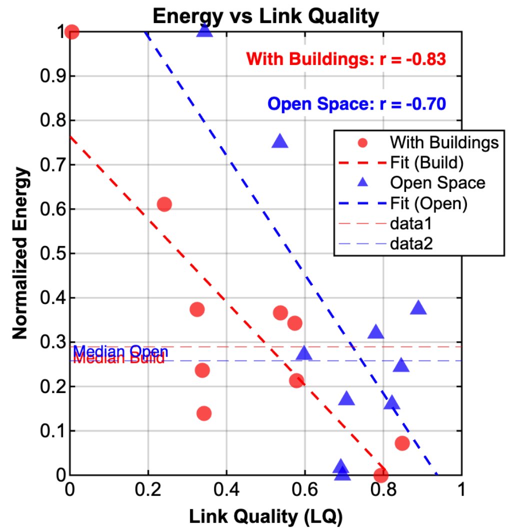

Fig. 4 ***Analysis of Normalised Energy vs Link Quality across both environments***

In the above Figure 4, the key relationship is that as the link quality increases, the normalised energy required reduces. This trend holds for both the simulations in the open and building environments. The key difference, however, is that for a constant link quality, the line of best fit for the building environment is lower than the line of best fit for the open environment. This is surprising as it would be expected that the energy usage would be lower for an open region rather than one with paths blocked by buildings. The median energy shown by the dimmer dotted lines in Figure 4 as well support this as the median energy for open is less than the median energy for buildings. This phenomenon is likely due to the fact that to achieve a certain link quality in building environments, the paths must be more strictly routed involving shorter and energy efficient paths. Open hops could have longer paths resulting in greater propulsion energy being required. Additionally there may be a greater exposure to wind in the open environment as there are no buildings to provide the shielding effect. Therefore energy is not needed to change positions but actually invested into stabilising the drone when faced with crosswinds. Therefore if data transferred is optimised in drone swarms, energy efficiency can be greatly improved especially in situations where the swarms are scattered in a crowded environment.

3.5. Analysis of Delay vs Normalised Energy across both environments

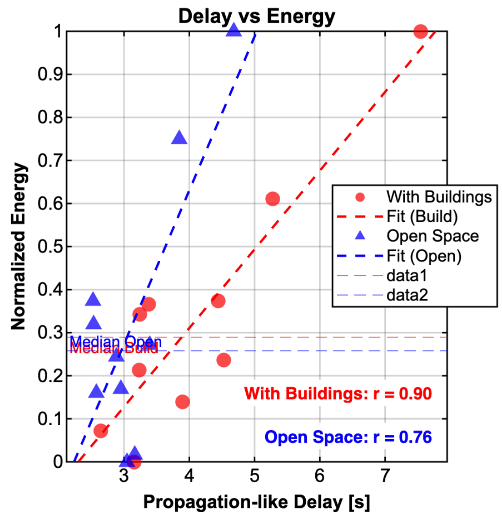

Fig. 5 Analysis of Delay vs Normalised Energy across both environments

Secondly, the normalised energy usage is compared against the propagation delay as seen in Figure 5. There is a positive relationship observed here for both environments and for a fixed delay the normalised energy usage for the open environment always exceeds the normalised energy usage for the building environment. As the propagation delay increases, the normalised energy consumed also increases. A longer delay is generally caused through longer or more complex paths therefore increasing the normalised energy in most cases. The reason for the open environment always using more energy than the building environment for a fixed propagation delay is due to the open environment having longer paths as mentioned before. With buildings, drones prefer to take shorter paths and this leads to lower energy consumed despite the same delay. This trend held true for all drones in the simulations as compared to the open and urban environments. The normalized energy consumption in the urban environment was lower for similar propagation delays as the routing paths were shorter and the surrounding buildings provided partial shield from crosswind.The urban environment consistently showed lower normalized energy consumption for similar propagation delays, because routing paths were shorter, and the crosswind was partially shielded by other buildings. The results indicate that energy efficiency can be higher in urban than in open environments, at least in certain cases, under the conditions assumed in the present model, even if the physical obstructions are present. These results show that in some cases placing drones in a building environment may actually be more energy-efficient than open environments due to the difference in types of paths.

3.6. Analysis of Communication Delay vs Link Quality across both environments

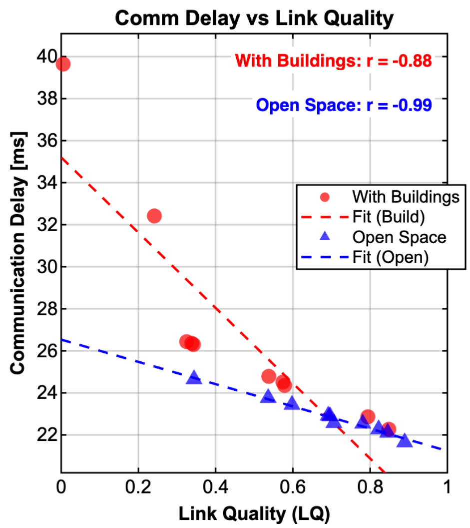

Fig. 6 Analysis of Communication Delay vs Link Quality across both environments

As seen in Figure 6, when communication delay is plotted against link quality, there is a negative correlation. As the link quality rises, the communication delay will reduce. This is a direct result of the formula used in Equation 13. As the link quality increases, the SNR is increased as well allowing more data packets to be transmitted in a lesser amount of time. Additionally Figure 6 shows that the gradient of the best fit line of the building environment is greater than the gradient of the best fit line of the open environments suggesting that a fixed amount increase in link quality causes a greater decrease in delay for the building environment as compared to the open environment. This occurs due to the links operating in capacity-limited regimes in urban environments where the SNR is generally lower. This is why when there is a marginal increase in the link quality, the throughput gains increase by a larger amount which leads to a larger delay. The same applies for the open scenario which operates with a generally higher SNR. So if the delay is to marginally increase, then the throughput gains would increase by a smaller amount causing a smaller decrease in delay.

CONCLUSION

Reliable and energy efficient data transmission is a pressing issue to UAV swarms that are used in complex three dimensional settings, especially when they are subject to atmospheric anomalies like cross winds[17]. The presence of urban structures and dynamic wind conditions adds a lot of variability to communication quality, latency and energy consumption, making it difficult to make routing decisions in the swarm. The paper addresses these challenges by investigating multi-objective routing for UAV swarms in 3D environments using Ant Colony Optimization (ACO), with explicit consideration of link quality, communication delay, and energy usage.

The current study discusses the effective communication between data transfer in a UAV swarm in an open environment and in a building-dense environment under the influence of crosswinds. The proposed model is realistic in that it considers three-dimensional mobility and environmental constraints in the operational environment experienced in actual deployment of UAV. The multi-objective routing in the dynamic aerial networks can be fully framed using ACO to optimize simultaneously link quality, communication delay, and energy consumption.

The results demonstrate that both environmental structure and wind conditions significantly influence routing decisions within the swarm. The ACO algorithm, in building-dense environments, has always prevented roof-grazing links [18], which led to lower link quality and higher propagation delay caused by attenuation caused by obstructions and off-line-of-sight communication routes. Nevertheless, there was still a similar amount of energy use in the open and built-in environments, which implied that the propulsion energy is the dominant constituent of the overall energy spending. This is an indication that the algorithm is able to overcome communication obstructions because it chooses shorter and more energy-efficient routes. Moreover, the presence of buildings also had an indirect beneficial impact on energy efficiency by partially shielding against cross winds and thus minimizing the wind induced propulsion penalties.

The findings also revealed some significant relationships between link quality, delay and energy consumption across both environments. There was a negative relationship between quality of link and delay of communication suggesting that the stronger the link the lower is the transmission delay. On the other hand positive correlation was found between energy consumption and propagation delay, as a manifestation of high energy requirements of long communication routes and manoeuvre requirements. Also, with the same quality of the links, or delay, UAVs in buildings tended to consume less energy than in open spaces, which emphasizes the unintuitive nature of environmental limitations on swarm operation and cost-effectiveness.

There are a number of avenues to make the proposed model more efficient and accurate. More ACO iterations may result in better convergence of pheromones into more consistent and global optimal routing paths especially in 3D urban environments, where the obstructions and wind penalties cause complex decision making dynamics. Additional refinements would be possible by adapting the ACO weighting parameters on the link quality, delay and energy consumption, ensuring the model becomes more robust across varying scenarios. Additional wind profiles, wind direction, and swarm size could also be investigated as the future work to assess the scalability and broaden the application of the framework.

Compared to previously existing UAV swarm routing and optimisation models, which predominantly focus on 2D environments [19], static link assumptions, or single objective optimisation, this work advances the state of art by incorporating 3 dimensional environment, crosswind induced energy penalties, and multi objective routing within the Ant Colony Optimisation framework. While prior studies demonstrate improvement in energy efficiency and delay minimisation in open environments, they often fail to consider the combined effects of urban structure and atmospheric conditions on inter-UAV communication. The proposed framework is well suited for practical applications of UAV swarms like disaster response, urban monitoring, infrastructure inspection, precision agriculture and search and rescue missions where reliable communication in a complex 3D environment is key for swarm coordination that requires robust, energy efficient and low latency communication.

AUTHOR'S CONTRIBUTIONS

Vedansh Gupta conceptualised the study, did literature survey, carried out simulations, analysed the data, wrote and corrected the manuscript.

CONFLICT OF INTEREST

The authors report no conflict of interest.

FUNDING

No funding information to disclose.

ACKNOWLEDGEMENTS

The authors would also acknowledge the use of Matlab to help with simulations and graphs presented. I would like to thank Mr. Arbaz Reza, Director of Accelo Mobility for guidance in this project.

REFERENCES

[1] K. Saleem and I. Ahmad, "Ant colony optimization (ACO) based autonomous secure routing protocol for mobile surveillance systems," *Drones*, vol. 6, no. 11, p. 351, 2022. [CrossRef] [Google Scholar] [Publisher Link]

[2] Yalavarthi A. K. A., Yalavarthi R., Saisandeep T., Sai S., Sha A., and Udayan D., "ACO-DTSP algorithm: Optimizing UAV swarm routes with workload constraints," *Procedia Computer Science*, vol. 235, pp. 163–172, 2024. [CrossRef] [Google Scholar] [Publisher Link]

[3] M. Kaur, A. Kaur, and P. Singh, "UAV swarm clustering and trajectory planning: A taxonomy, systematic review, current trends and research challenges," *Computers and Electrical Engineering*, vol. 128, p. 110697, 2025. [CrossRef] [Google Scholar] [Publisher Link]

[4] E. Yucesoy, B. Balcik, and E. Coban, "The role of drones in disaster response: A literature review of operations research applications," *International Transactions in Operational Research*, vol. 32, no. 2, 2024. [CrossRef] [Google Scholar] [Publisher Link]

[5] A. Fascista, "Toward integrated large-scale environmental monitoring using WSN/UAV/crowdsensing: A review of applications, signal processing, and future perspectives," *Sensors*, vol. 22, no. 5, p. 1824, 2022. [CrossRef] [Google Scholar] [Publisher Link]

[6] D. C. Tsouros, S. Bibi, and P. G. Sarigiannidis, "A review on UAV-based applications for precision agriculture," *Information*, vol. 10, no. 11, p. 349, 2019. [CrossRef] [Google Scholar] [Publisher Link]

[7] I. Munasinghe, A. Perera, and R. C. Deo, "A comprehensive review of UAV-UGV collaboration: Advancements and challenges," *Journal of Sensor and Actuator Networks*, vol. 13, no. 6, p. 81, 2024. [CrossRef] [Google Scholar] [Publisher Link]

[8] D. Clerigues, J. Wubben, C. T. Calafate, J.-C. Cano, and P. Manzoni, "Enabling resilient UAV swarms through multi-hop wireless communications," *EURASIP Journal on Wireless Communications and Networking*, vol. 2024, no. 1, 2024. [CrossRef] [Google Scholar] [Publisher Link]

[9] D. Nar and R. Kotecha, "Optimal waypoint assignment for designing drone light show formations," *Results in Control and Optimization*, vol. 9, p. 100174, 2022. [CrossRef] [Google Scholar] [Publisher Link]

[10] A. M. Raivi, S. M. A. Huda, M. M. Alam, and S. Moh, "Drone routing for drone-based delivery systems: A review of trajectory planning, charging, and security," *Sensors*, vol. 23, no. 3, p. 1463, 2023. [CrossRef] [Google Scholar] [Publisher Link]

[11] A. Tahir, J. Böling, M.-H. Haghbayan, H. T. Toivonen, and J. Plosila, "Swarms of unmanned aerial vehicles — A survey," *Journal of Industrial Information Integration*, vol. 16, Art. no. 100106, 2019. [CrossRef] [Google Scholar] [Publisher Link]

[12] H. T. Friis, "A note on a simple transmission formula," *Proceedings of the IRE*, 1946. [CrossRef] [Google Scholar] [Publisher Link]

[13] International Telecommunication Union, "Calculation of free-space attenuation (Recommendation ITU-R P.525-5)," ITU-R, Geneva, Switzerland, Technical Report, 2024.

[14] C. E. Shannon, "A mathematical theory of communication," *Bell System Technical Journal*, vol. 27, pp. 379–423, 623–656, 1948. [CrossRef] [Google Scholar] [Publisher Link]

[15] R. D'Andrea, "Can drones deliver?" *IEEE Transactions on Automation Science and Engineering*, vol. 11, no. 3, pp. 647–648, 2014. [CrossRef] [Google Scholar] [Publisher Link]

[16] C. Briso, C. Calvo, Z. Cui, L. Zhang, and Y. Xu, "Propagation measurements and modeling for low altitude UAVs from 1 to 24 GHz," *arXiv*, arXiv:2502.17444, 2025. [CrossRef] [Google Scholar] [Publisher link]

[17] R. Gu, Y. Zhao, and X. Ren, "Integrating wind field analysis in UAV path planning: Enhancing safety and energy efficiency for urban logistics," *Chinese Journal of Aeronautics*, vol. 39, no. 1, p. 103605, 2026. [CrossRef] [Google Scholar] [Publisher Link]

[18] A. Mohamed, M. Marino, S. Watkins, J. Jaworski, and A. Jones, "Gusts encountered by flying vehicles in proximity to buildings," *Drones*, vol. 7, no. 1, p. 22, 2023. [CrossRef] [Google Scholar] [Publisher Link]

[19] D. G. Gioia, J. Bonari, D. Lichte, and A. Popp, "Sequential drone routing for data assimilation on a 2D airborne contaminant dispersion problem," *arXiv*, arXiv:2410.10346, 2024. [CrossRef] [Google Scholar] [Publisher Link]